

Synthesis and biological evaluation of RGD peptides with the $^{99m}\text{Tc}/^{188}\text{Re}$ chelated iminodiacetate core: highly enhanced uptake and excretion kinetics of theranostics against tumor angiogenesis†

Cite this: *RSC Advances*, 2013, 3, 782

Byung Chul Lee,^a Byung Seok Moon,^a Ji Sun Kim,^a Jae Ho Jung,^a Hyun Soo Park,^a John A. Katzenellenbogen^b and Sang Eun Kim^{*ac}

To develop a companion set of RGD-based agents for diagnostic and radiotherapeutic purposes, facile incorporation of $^{99m}\text{Tc}(\text{CO})_3$ or $^{188}\text{Re}(\text{CO})_3$ into the same precursor produced, respectively, a structurally and functionally matched radiodiagnostic and radiotherapeutic—or theranostic—pair. This work presents the synthesis of two ^{99m}Tc -labeled RGD monomers (**4** and **5**) along with a ^{99m}Tc -labeled RGD dimer (**6**) and an investigation of the influence of the small-sized and negatively charged ^{99m}Tc -iminodiacetate (IDA) core on the *in vitro* and *in vivo* behavior of these three different RGD analogs for imaging integrin $\alpha_v\beta_3$ expression. Among the three ^{99m}Tc -IDA-RGD analogs, **6** exhibited the highest integrin binding affinity with an IC_{50} value of 0.5 nM and a tumor uptake with an ID/g value of $12.3 \pm 5.15\%$ at 60 min post-injection, whereas liver and intestinal levels remained relatively low with good metabolic stability ($>97\%$), presumably because of the overall negative charge of the radiometal chelating system. Both $^{99m}\text{Tc}/^{188}\text{Re}$ -labeled compounds (**6** and **7**), which were prepared from the precursor (**18**), provided a good tumor accumulation and a clearly visible image of the tumor with high contrast, as compared to the contralateral background in the U87-MG xenograft model. These data support the use of ^{99m}Tc - and ^{188}Re -IDA-D-[c(RGDfK)]₂ as a matched radio-theragnostic pair that can be used to individualize radiotherapy for angiogenesis-dependent cancer.

Received 9th October 2012,
Accepted 7th November 2012

DOI: 10.1039/c2ra22460g

www.rsc.org/advances

Introduction

Targeted tumor-angiogenesis imaging can provide early diagnosis, aid in treatment planning and monitoring of anti-angiogenic therapies in cancer.^{1,2} Integrin $\alpha_v\beta_3$ is a suitable target for both tumor-angiogenesis imaging and anti-angiogenic therapy because it is highly expressed on activated endothelial cells and new blood vessels found in tumors and surrounding tissues but absent in most organs.³ Interest in tumor-induced angiogenesis has increased enormously over the past decade, and it is known that the binding region in integrin $\alpha_v\beta_3$ contains the tripeptide sequence of arginine-glycine-aspartic acid derivatives, commonly known as

“RGD”.^{4,5} RGD analogs have been widely investigated and shown to be valuable tools for targeted tumor angiogenesis imaging.^{6,7} Single photon emission computed tomography (SPECT)/computed tomography (CT) is a non-invasive imaging modality that can longitudinally diagnose the target environment in the same animal across different time-points, and RGD analogs can be potentially combined with SPECT/CT for diagnostic purposes. We focused on the radionuclides ^{99m}Tc and ^{188}Re , respectively, to develop a companion set of RGD-based agents for diagnostic and radiotherapeutic purposes. ^{99m}Tc is desirable for diagnostic imaging because of its ideal nuclear properties ($t_{1/2} = 6$ h, 141 keV), while ^{188}Re , with a half-life of 17 h and a maximum beta energy of 2.12 MeV, is favorable for tumor radiotherapy. Moreover, both ^{99m}Tc and ^{188}Re are readily obtained by daily elution from $^{99}\text{Mo}/^{99m}\text{Tc}$ - and $^{188}\text{W}/^{188}\text{Re}$ -generator, respectively, and are thus very convenient and suitable for routine clinical use. Over the past decade, other research groups have tried to synthesize ^{99m}Tc -labeled RGD analogs containing various ^{99m}Tc chelating moieties, such as 2-mercaptoacetyl-glycylglycyl (MAG₂), 6-hydrazinonicotinamide (HYNIC), nitrido-core and the 4 + 1 mixed ligand system.^{8,9} However, these ^{99m}Tc chelating

^aDepartment of Nuclear Medicine, Seoul National University Bundang Hospital, Seoul National University College of Medicine, 300 Gumidong, Bundanggu, Seongnam 463-707, Republic of Korea. E-mail: kse@snu.ac.kr; Fax: 82-31-787-4018; Tel: 82-31-787-7671

^bDepartment of Chemistry, University of Illinois, Urbana, Illinois 61801, USA

^cProgram in Biomedical Radiation Sciences, Department of Transdisciplinary Studies, Graduate School of Convergence Science and Technology, Seoul National University, Seoul 151-742, Korea

† Electronic supplementary information (ESI) available. See DOI: 10.1039/c2ra22460g

moieties of a targeted compound have significant shortcomings, *i.e.*, a bulky core size, low metabolic stability and slow clearance from normal tissue. Therefore, certain RGD analogs have been formulated to include polyethylene glycol (PEG₄) or glycine (G₃) linkers to increase the integrin $\alpha_v\beta_3$ binding affinity in a “bivalent” fashion and to improve radiotracer excretion kinetics from normal organs.¹⁰

Recently, the tricarbonyl technetium-99m (^{99m}Tc-(CO)₃) unit has been shown to be useful for introducing ^{99m}Tc into biomolecules because of its high chemical stability and small size. The *fac*-[^{99m}Tc(H₂O)₃(CO)₃]⁺ synthon can be readily generated from ^{99m}TcO₄⁻ and CO gas in the presence of NaBH₄.^{11,12} Additionally, therapeutic radionuclides such as β -emitting rhenium-188 [¹⁸⁸Re(H₂O)₃(CO)₃]⁺ also could be prepared from the same class of ligands used for chelation of the [^{99m}Tc(H₂O)₃(CO)₃]⁺ moiety.¹³

Many small ^{99m}Tc-(CO)₃ cores (^{99m}Tc(I)-complex) with tridentate ligands have been developed and used for the preparation of ^{99m}Tc-(CO)₃-labeled radiotracers.^{14–19} We have also previously reported the use of ^{99m}Tc-labeled glucosamino-D-c(RGDfK) that includes a ^{99m}Tc(CO)₃-(iminodiacetate, IDA) core as a new radiotracer for tumor angiogenesis imaging.^{20,21} Although ^{99m}Tc-labeled glucosamino-D-c(RGDfK) had a high integrin binding affinity *in vitro*, this radiotracer was not useful as a diagnostic agent because of its low tumor uptake *in vivo*. We hypothesized that the overall negative charge of the radiometal interacted with the nearby positive charge of arginine in the RGD peptide, thus interfering with the binding of the peptide unit to the integrin target *in vivo*. However, including a negative charge in the ^{99m}Tc core could lead to the development of new analogs having improved biodistribution as well as desirable pharmacokinetic properties.²²

As a continuation of our interest in ^{99m}Tc-(CO)₃-labeled RGD peptides with a negative charge on the ^{99m}Tc-(CO)₃ core, we designed two ^{99m}Tc-labeled RGD monomers with or without a PEG chain (**4** and **5**), along with a ^{99m}Tc-labeled RGD dimer (**6**), and evaluated *in vitro* and *in vivo* their capacity to image integrin $\alpha_v\beta_3$ expression. Accordingly, a ¹⁸⁸Re-labeled RGD analog (**7**) was prepared for a radiotherapeutic purpose from the selected precursor. Our goal was to develop a companion set of RGD-based agents (radio-theranostics), which incorporated tricarbonyl ^{99m}Tc or ¹⁸⁸Re complexes into the same precursor, with the choice of radionuclide determining the potential diagnostic and therapeutic utility.

Results and discussion

Chemical synthesis

We have focused on the development of a diagnostic imaging agent containing an RGD peptide for tumor angiogenesis, aiming to introduce the small-sized ^{99m}Tc-(CO)₃-IDA core into an RGD peptide in order to increase the hydrophilicity of the targeted molecule, and to do this, we have made a comparative evaluation of three ^{99m}Tc-IDA-RGD analogs (**4**, **5**, and **6**) in

terms of their tumor accumulation and pharmacokinetic properties.

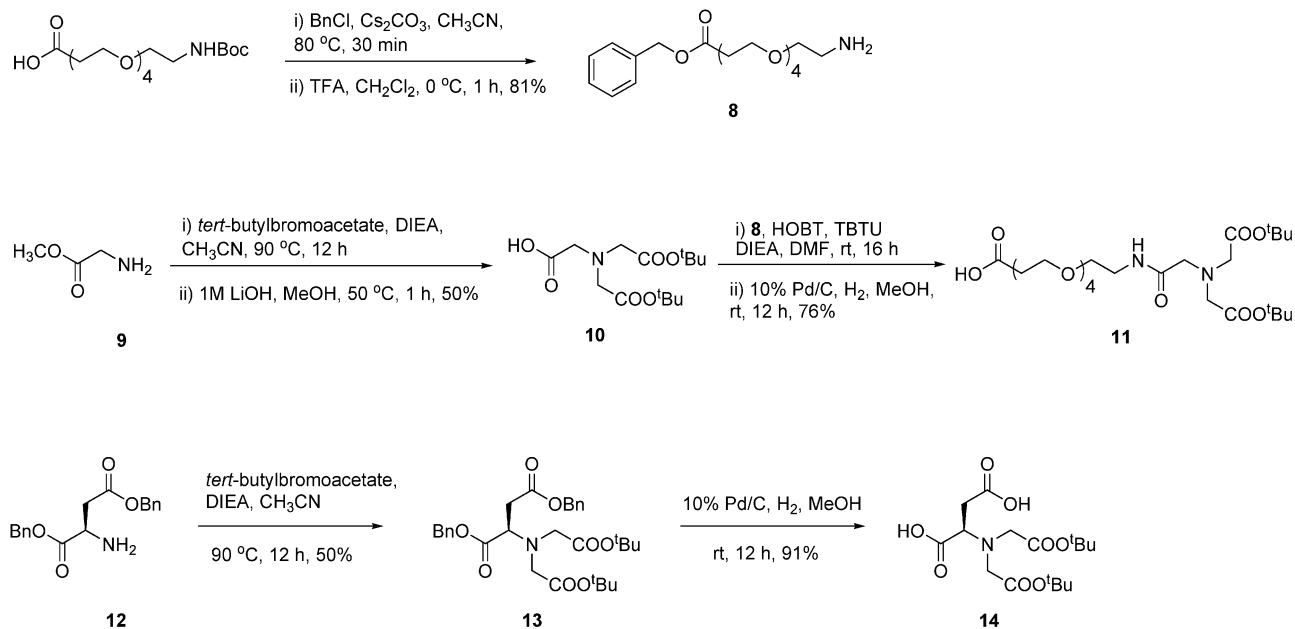
Synthesis of ^{185/187}Re-IDA-RGD analogs (1–3) and radiochemical synthesis of ^{99m}Tc/¹⁸⁸Re-IDA-RGD analogs (4–7)

Compound **8** was prepared from the Boc protected PEG acid and benzyl chloride in the presence of cesium carbonate, followed by acidic hydrolysis in a trifluoroacetic acid (TFA)–methylene chloride mixture, as summarized in Scheme 1. To introduce the ^{99m}Tc-(CO)₃-IDA core and PEG chain onto the lysine residue, treatment of glycine methyl ester **9** with *tert*-butyl bromoacetate in CH₃CN in the presence of DIEA, followed by hydrolysis with LiOH, resulted in the formation of the acid compound **10**. The amino group of compound **8** was linked with the acid compound **10** using an amide bond condensation and then, the IDA moiety linked PEG acid **11** was prepared in the presence of 10% palladium on charcoal within a hydrogen atmosphere. Compound **14** was synthesized using the same procedures described above as the introduction of an IDA moiety and deprotection of two benzyl groups at acid residues.

The small size of the ^{99m}Tc-(CO)₃-IDA core led us to design and synthesize three ^{99m}Tc-labeled RGD analogs as radiotracers for tumor angiogenesis. The ^{99m}Tc-labeled RGD monomer precursor **16**, IDA-c(RGDfK), for [^{99m}Tc(H₂O)₃(CO)₃]⁺ labeling, was synthesized by reacting *tert*-butyl bromoacetate with the free amine of lysine in the protected cyclic-R(Pbf)-G-D(OtBu)-f-K-NH₂ **15**, and the subsequent removal of *tert*-butyl and 2,2,4,6,7-pentamethyldihydrobenzofuran-5-sulfonyl (Pbf) groups on the side chains of the IDA moiety, aspartic acid and arginine. The ^{99m}Tc-labeled RGD monomer precursor with PEG chain **17** and ^{99m}Tc-labeled RGD dimer precursor **18** were prepared from **15** using an amide bond condensation with compound **11** and **14**, respectively, as shown in Scheme 2. Subsequently, the protecting groups, three *tert*-butyl and Pbf groups, were removed by the treatment of a mixture of TFA–HSC₂CH₂SH–H₂O (95 : 2.5 : 2.5) to obtain the desired precursors **16**, **17** and **18**. The “cold” rhenium coordination reaction with the precursors (**16**, **17**, or **18**) was performed in a water–methanol mixture (1 : 1) at 65 °C using (NEt₄)₂ [^{185/187}ReCl₃(CO)₃] (Scheme 2). The desired ^{185/187}Re(CO)₃ coordinated RGD-peptides were synthesized from each precursor (**16**, **17**, and **18**) in 60–78% yields and revealed HPLC retention times of 21.8 min for **1**, 22.1 min for **2** and 19.2 min for **3**. The reaction was monitored by HPLC until the precursor peak disappeared. Incorporation of ^{99m}Tc/¹⁸⁸Re-(CO)₃ into the IDA moiety in the precursors was performed in aqueous media. The overall radiochemical yields were 72–79% for **4**, **5** and **6** and 50–55% for **7**, and all compounds were obtained with high radiochemical purity (>95%).

In vitro integrin receptor-binding assay

As shown in Chart 1, the IC₅₀ values of the compounds suggested that the monomeric RGD analogs (**1** and **2**) had similar binding affinity values, while the dimeric RGD analog **3** possessed higher affinity than either of the monomeric RGD analogs, possibly because of the bivalency effect. Thus, it appears that the small size of the ^{185/187}Re-(CO)₃-IDA core introduced into the RGD analogs (**1**, **2**, and **3**) resulted in conjugates having high binding affinity for integrin-positive cells.

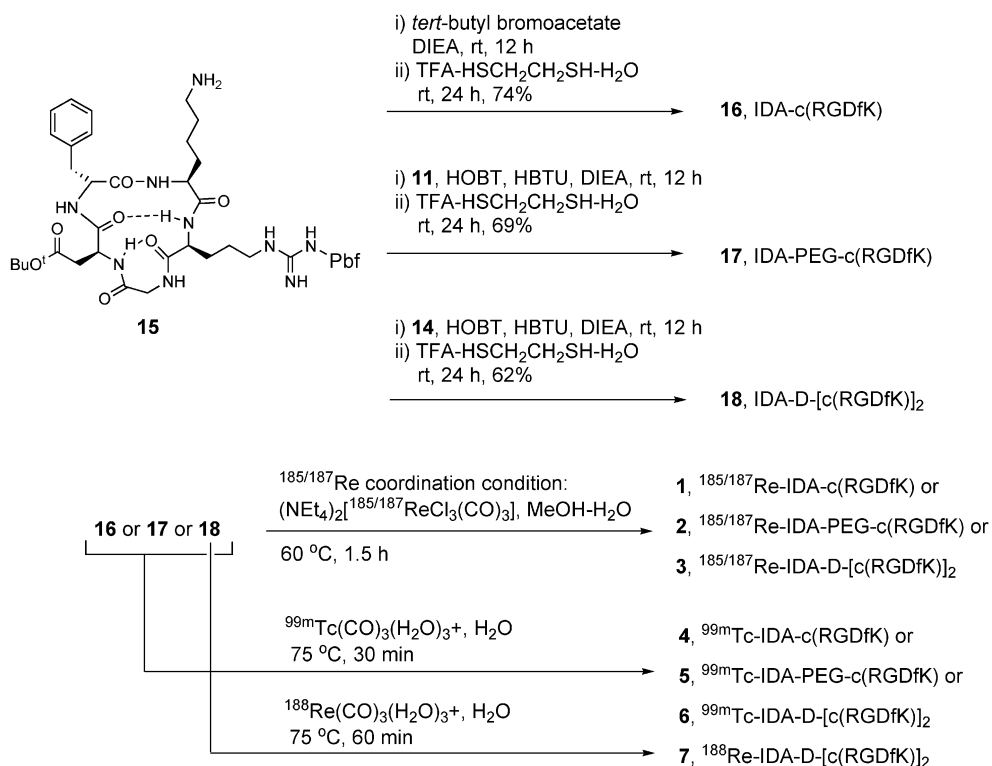


Scheme 1

Biodistribution studies

In *ex vivo* distribution studies, we used human glioblastoma U87-MG cells, an integrin $\alpha_v\beta_3$ -positive tumor cell line.^{23,24} Tumor cells were engrafted on the flanks of Balb/c nude mice. After tumor volume reached approximately $62.8 \pm 16.8 \text{ mm}^3$,

the three ^{99m}Tc -IDA-RGD analogs (**4**, **5**, and **6**) were administered intravenously, and at various time points thereafter, mice were sacrificed to perform tissue distribution studies (Table 1).



Scheme 2

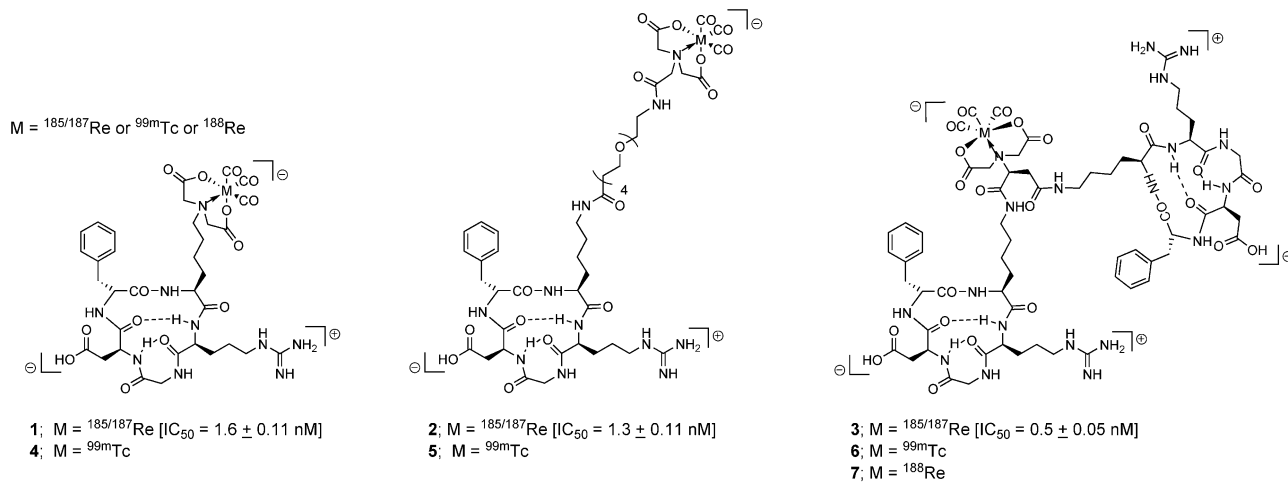


Chart 1

The blood levels of both peptides 5 and 6 were around 0.6% ID/g (30 min post-injection), whereas that of 4 is even lower with rapid clearance in the blood. The tumor radioactivity levels of the three $^{99\text{m}}\text{Tc}$ -labeled RGD analogs at 60 min post-injection were $0.40 \pm 0.14\%$ ID/g (4), $3.35 \pm 1.23\%$ ID/g (5), and $12.3 \pm 5.15\%$ ID/g (6), respectively. Although 4 has a relatively high receptor binding affinity, the additional negative charge in the RGD analog 4 led to an unfavorable biodistribution *in vivo*. This lack of correlation between receptor binding affinity and tumor accumulation may be due to the polarity-dependent tumor penetration and the binding affinity for the receptors, as reported for other radiolabeled peptides.²² We also had anticipated that the negatively charged $^{99\text{m}}\text{Tc}$ -(CO)₃-IDA core might induce unwanted interactions with the positive charge of the arginine residue, thus reducing the affinity of the integrin-binding *in vivo*. Our previously reported RGD analogs, $^{99\text{m}}\text{Tc}$ -labeled glucosamino-D-c(RGDfK) containing the $^{99\text{m}}\text{Tc}$ -(CO)₃-IDA core, also showed similar poor biodistribution profiles.²⁰ Among other reported $^{99\text{m}}\text{Tc}$ -(CO)₃-labeled RGD analogs, the $^{99\text{m}}\text{Tc}$ -(CO)₃-pyrazolyl conjugate of c(RGDyK), which simply linked the positive-charge core through the side arm of the lysine residue, showed relatively high tumor and liver uptake compared to 4, which contained the negative charge on the $^{99\text{m}}\text{Tc}$ core.¹⁶

To avoid the undesirable interaction between the $^{99\text{m}}\text{Tc}$ -(CO)₃-IDA core and the arginine, we inserted a PEG linker on the side arm of the lysine in the RGD analog. The uptake of $^{99\text{m}}\text{Tc}$ -IDA-PEG-c(RGDfK) (5) in integrin-positive tumor cells was similar to other monomeric RGD analogs, with slightly faster clearance from normal organs than the positive charge-containing $^{99\text{m}}\text{Tc}$ -(CO)₃-pyrazolyl conjugate of c(RGDyK). The liver uptake of both peptides 5 and 6 was similar at 30 min post-injection; however, the intestinal uptake of 6 was gradually reduced to significantly lower levels than that of 5 at 240 min post-injection. Remarkably, the tumor uptake of $^{99\text{m}}\text{Tc}$ -IDA-D-[c(RGDfK)]₂ (6) was rapid and high, whereas its liver and intestinal levels remained relatively low. Thus, over time, the tumor-to-liver ratios of 6 increased from 4.0 at 10 min post-injection to a peak of 5.2 at 1 h, which was maintained until 4 h.

Finally, we selected the dimeric cRGD precursor 18 and introduced the ^{188}Re -(CO)₃-IDA core as the therapeutic agent. The radiochemical synthesis of [$^{188}\text{Re}(\text{CO})_3(\text{H}_2\text{O})_3$]⁺ was performed as previously described.¹³ The highest tumor radioactivity level of 7 was $12.3 \pm 1.7\%$ ID/g at 30 min post-injection. The liver uptake of both peptides was similar at 30 min post-injection, whereas liver uptake of 7 gradually became lower than that of 6 by 2 h. Over time, tumor-to-liver ratios of 7 increased continuously to 11.2 until 8 h. Thus, *ex vivo* biodistribution demonstrated that the matched pair of $^{99\text{m}}\text{Tc}$ and ^{188}Re -labeled peptides (6 and 7) have both similar and very high integrin binding affinity in a tumor xenograft.

SPECT/CT imaging studies in U87-MG tumor-bearing mice

As shown in Fig. 1, comparison of the SPECT/CT images of the three $^{99\text{m}}\text{Tc}$ -IDA-RGD analogs and ^{188}Re -IDA-D-[c(RGDfK)]₂ visually reflected the *ex vivo* biodistribution of $^{99\text{m}}\text{Tc}$ / ^{188}Re uptake in the animal model. All the $^{99\text{m}}\text{Tc}$ -IDA-RGD analogs showed rapid clearance from the blood after injection, and the major radioactivity was excreted in the urine (Fig. 1). The introduction of the spacer in 5 significantly influenced tumor accumulation. Among the four analogs examined here, 6 and 7 possessed high tumor uptake as well as low liver and intestinal uptake. The higher kidney uptake is probably caused by the increased arginine residues. This influence of the positive charge on the renal uptake has been reported for radiolabeled multimeric cyclic RGD peptides and other peptides.^{10,25} On the basis of both high tumor uptake and low uptake in receptor-negative tissues of 6 and 7, we believe that low uptake and rapid reduction in hepatic levels might be the result of rapid renal clearance engendered by the negative charge on the $^{99\text{m}}\text{Tc}$ / ^{188}Re -(CO)₃-IDA core attached to the RGD peptide dimer. These results indicate that modification of the polarity with a single negative charge can change the pharmacokinetics and have a desirable effect on the biodistribution of biomolecules. The diminutive and hydrophilic $^{99\text{m}}\text{Tc}$ / ^{188}Re -(CO)₃-IDA core is expected to only minimally perturb the biological activity of RGD, with subsequently increased tumor targeting and improved *in vivo* kinetics.

Table 1 *Ex vivo* biodistribution studies (% ID/g \pm SD)^a of ^{99m}Tc-IDA-RGD analogs^b (**4–7**) in U87-MG xenografts

^{99m} Tc-IDA-c(RGDfK), 4					
Tissue/organ	10 min	30 min	60 min	120 min	240 min
Blood	0.37 \pm 0.04	0.10 \pm 0.01	0.03 \pm 0.00	0.02 \pm 0.00	—
Liver	5.12 \pm 0.76	0.92 \pm 0.10	0.45 \pm 0.09	0.30 \pm 0.09	—
Lung	1.72 \pm 0.86	0.54 \pm 0.14	0.27 \pm 0.07	0.40 \pm 0.46	—
Spleen	0.56 \pm 0.32	0.19 \pm 0.10	0.12 \pm 0.03	0.08 \pm 0.03	—
Kidneys	1.65 \pm 0.48	0.50 \pm 0.09	0.23 \pm 0.02	0.13 \pm 0.01	—
Small intestine	4.41 \pm 1.00	5.59 \pm 0.86	3.95 \pm 0.22	4.00 \pm 0.41	—
Large intestine	0.55 \pm 0.37	0.31 \pm 0.06	0.53 \pm 0.81	0.11 \pm 0.01	—
Thyroid	0.05 \pm 0.02	0.01 \pm 0.00	0.01 \pm 0.00	0.03 \pm 0.03	—
Muscle	0.56 \pm 0.27	0.16 \pm 0.04	0.08 \pm 0.07	0.05 \pm 0.02	—
Brain	0.04 \pm 0.01	0.02 \pm 0.00	0.01 \pm 0.01	0.03 \pm 0.02	—
Tumor	1.43 \pm 0.15	0.78 \pm 0.40	0.40 \pm 0.14	0.33 \pm 0.06	—
^{99m} Tc-IDA-PEG-c(RGDfK), 5					
Tissue/organ	10 min	30 min	60 min	120 min	240 min
Blood	1.43 \pm 0.23	0.66 \pm 0.09	0.35 \pm 0.06	0.17 \pm 0.02	0.11 \pm 0.01
Liver	5.30 \pm 0.95	2.62 \pm 0.28	1.41 \pm 0.21	0.98 \pm 0.15	0.64 \pm 0.08
Lung	3.50 \pm 0.18	2.87 \pm 0.56	1.52 \pm 0.19	0.65 \pm 0.08	0.32 \pm 0.04
Spleen	2.31 \pm 0.36	1.45 \pm 0.18	0.77 \pm 0.07	0.47 \pm 0.10	0.20 \pm 0.02
Kidneys	7.53 \pm 0.46	4.33 \pm 1.60	2.80 \pm 0.89	1.13 \pm 0.11	0.61 \pm 0.14
Small intestine	17.6 \pm 2.20	15.6 \pm 2.89	4.79 \pm 2.13	2.77 \pm 0.96	0.37 \pm 0.17
Large intestine	2.06 \pm 0.25	1.21 \pm 0.20	0.98 \pm 0.30	26.8 \pm 2.80	28.1 \pm 5.82
Thyroid	0.20 \pm 0.04	0.12 \pm 0.03	0.08 \pm 0.02	0.03 \pm 0.00	0.01 \pm 0.01
Muscle	1.31 \pm 0.02	0.97 \pm 0.19	0.66 \pm 0.13	0.52 \pm 0.47	0.07 \pm 0.01
Brain	0.10 \pm 0.01	0.07 \pm 0.01	0.06 \pm 0.01	0.04 \pm 0.02	0.02 \pm 0.00
Tumor	5.43 \pm 0.50	4.27 \pm 1.15	3.35 \pm 1.23	2.63 \pm 0.74	1.41 \pm 0.24
^{99m} Tc-IDA-D-[c(RGDfK)] ₂ , 6					
Tissue/organ	10 min	30 min	60 min	120 min	240 min
Blood	1.16 \pm 0.08	0.62 \pm 0.11	0.42 \pm 0.01	0.26 \pm 0.05	0.16 \pm 0.02
Liver	3.10 \pm 0.58	2.24 \pm 0.33	2.36 \pm 0.21	2.06 \pm 0.54	1.24 \pm 0.19
Lung	4.34 \pm 0.69	3.34 \pm 0.80	3.55 \pm 0.26	2.19 \pm 0.35	1.33 \pm 0.09
Spleen	3.33 \pm 0.89	2.67 \pm 0.63	2.92 \pm 0.29	2.12 \pm 0.32	1.29 \pm 0.21
Kidneys	11.5 \pm 1.36	10.9 \pm 1.71	12.1 \pm 1.62	10.1 \pm 2.82	7.14 \pm 0.85
Small intestine	5.82 \pm 0.08	4.10 \pm 1.09	3.90 \pm 0.48	2.85 \pm 0.99	1.62 \pm 0.18
Large intestine	4.42 \pm 0.85	3.93 \pm 0.57	4.08 \pm 0.53	2.63 \pm 0.84	1.54 \pm 0.20
Thyroid	0.19 \pm 0.03	0.15 \pm 0.02	0.14 \pm 0.03	0.12 \pm 0.04	0.10 \pm 0.02
Muscle	1.48 \pm 0.21	1.49 \pm 0.44	2.23 \pm 1.44	1.11 \pm 0.43	0.64 \pm 0.07
Brain	0.13 \pm 0.02	0.10 \pm 0.02	0.10 \pm 0.01	0.08 \pm 0.01	0.06 \pm 0.01
Tumor	12.4 \pm 3.89	11.5 \pm 1.53	12.3 \pm 5.15	9.81 \pm 1.92	6.15 \pm 0.84
¹⁸⁸ Re-IDA-D-[c(RGDfK)] ₂ , 7					
Tissue/organ	10 min	30 min	60 min	120 min	480 min
Blood	1.13 \pm 0.18	0.58 \pm 0.02	0.33 \pm 0.04	0.10 \pm 0.02	0.03 \pm 0.00
Liver	3.77 \pm 0.13	2.58 \pm 0.26	1.78 \pm 0.34	1.07 \pm 0.18	0.35 \pm 0.05
Lung	4.52 \pm 0.76	3.56 \pm 0.37	2.68 \pm 0.66	1.41 \pm 0.12	0.67 \pm 0.07
Spleen	3.30 \pm 0.48	2.81 \pm 0.67	1.66 \pm 1.01	1.39 \pm 0.24	0.70 \pm 0.15
Kidneys	11.8 \pm 0.74	9.25 \pm 1.24	7.88 \pm 1.40	6.11 \pm 0.76	3.30 \pm 0.42
Small intestine	3.68 \pm 0.36	3.14 \pm 0.90	2.95 \pm 0.63	1.81 \pm 0.16	0.86 \pm 0.07
Large intestine	2.14 \pm 0.41	1.16 \pm 0.20	1.10 \pm 0.12	1.77 \pm 0.27	4.49 \pm 0.58
Thyroid	0.22 \pm 0.10	0.21 \pm 0.16	0.13 \pm 0.03	0.07 \pm 0.01	0.05 \pm 0.01
Muscle	1.58 \pm 0.14	1.17 \pm 0.36	1.02 \pm 0.24	0.71 \pm 0.18	0.33 \pm 0.03
Brain	0.19 \pm 0.04	0.14 \pm 0.06	0.10 \pm 0.02	0.06 \pm 0.00	0.04 \pm 0.01
Tumor	10.5 \pm 1.19	12.3 \pm 1.73	11.5 \pm 1.41	10.6 \pm 0.31	3.91 \pm 0.27

^a Percent of injected dose per gram of tissue; mean \pm SD ($n = 4$). ^b Tracer (**4**, **5**, **6**, or **7**) was dissolved in saline and injected into U87-MG-bearing nude mice. The dose per mouse was 0.74 MBq *via* the tail vein.

To confirm the receptor-binding specificity of **6**, a blocking experiment was performed. *In vivo* blocking with excess cRGDyV (18 mg kg⁻¹) resulted in significantly reduced radioactivity uptake in the tumor. In addition, the use of an integrin non-binding, negative control peptide, ^{99m}Tc-IDA-D-

[c(RADfK)]₂, indicated that the uptake of the major fraction of **6** in the tumor was selectively integrin-mediated, as shown in Fig. 2. This RAD peptide does not bind to integrin $\alpha_v\beta_3$, due to the addition of a single methyl group that results from changing glycine to alanine.²⁶

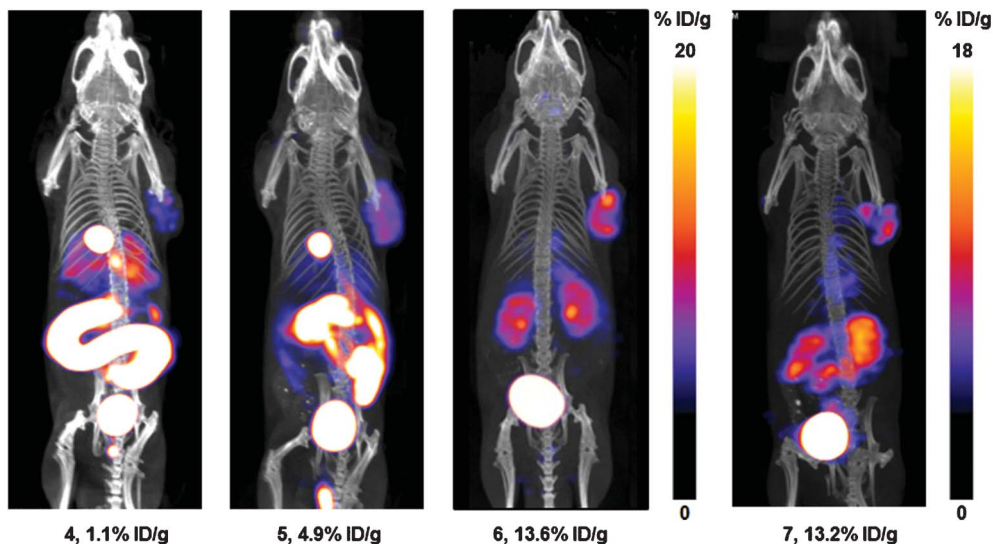


Fig. 1 Comparison of SPECT/CT images of ^{99m}Tc -IDA-RGD analogs (**4**, **5**, and **6**) and ^{188}Re -IDA-D-[c(RGDfK)]₂ (**7**).

Metabolic stability

In metabolic stability studies, the radioactivity in the tumor remained stable from 30 min until 2 h, with retained activity being over 98% for non-metabolized species; furthermore, the labeled peptides also remained stable in the other organs and

blood (Fig. 3). The metabolic stability of **6** was evaluated in human U87-MG glioma tumor-bearing nude mice and determined in blood and urine samples and in liver, kidneys, and tumor homogenates at 30 min, and 2 h each after intravenous injection. The extraction efficiency of all organs

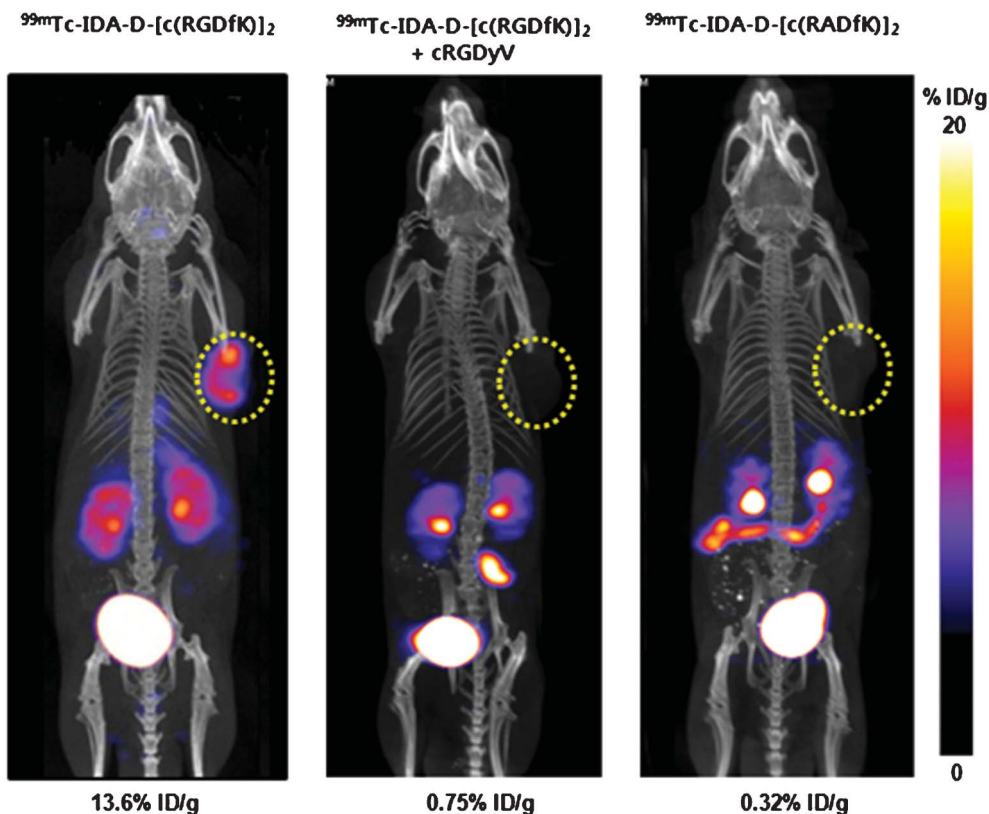


Fig. 2 SPECT/CT imaging of the tumor region with or without cRGDyV and SPECT/CT imaging of ^{99m}Tc -IDA-D-[c(RADfK)]₂ for a negative control peptide. Yellow circles indicate the tumor location. Color bars indicate the range of radio-uptake as a percentage of the injected dose per gram of tissue.

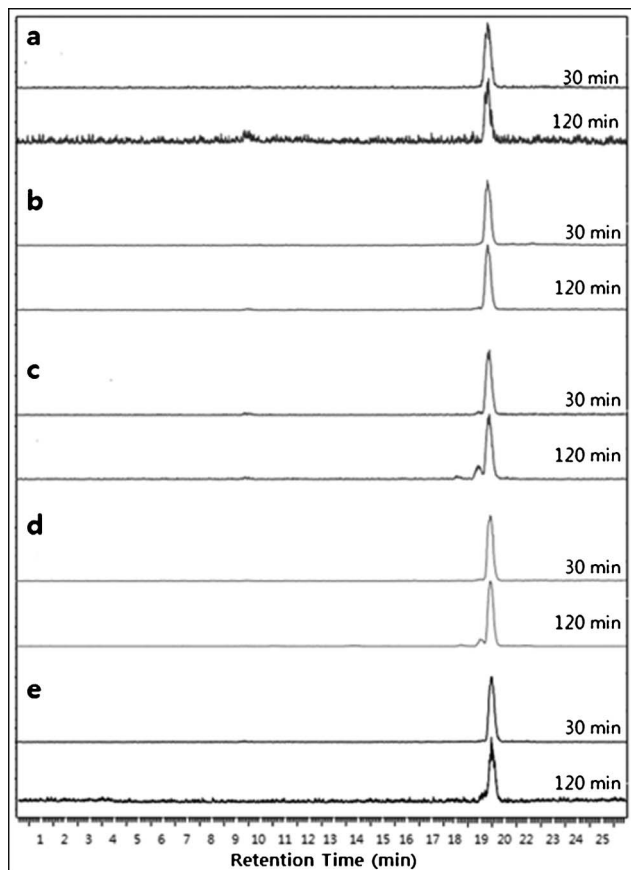


Fig. 3 Identification of parent and metabolites of **6** in a mouse xenograft model. HPLC profiles of each sample at 30 and 120 min post-injection: blood samples (a), urine samples (b), liver samples (c), kidney samples (d), and tumor samples (e).

was over 87% for 30 min post-injection, except for blood (Online Supplementary Information Table 2†). The retention time for **6** was 19.5 min. The HPLC profiles showed two metabolites having retention times of 9 and 19 min in the blood, liver, and kidneys. ^{99m}Tc -IDA-D-[c(RGDfK)]₂ reached stable levels in all the samples by 2 h after injection; however, some degradation was observed at later time points in the blood (19%), liver (18%), and kidneys (13%). The amount of intact tracer in the tumor was greater than 98% by 2 h.

These results indicate **6** to be a metabolically stable peptide that can monitor overexpressed integrin $\alpha_v\beta_3$ on newly formed blood vessels near and within tumor tissue. This agent can thus be potentially useful for monitoring the therapeutic anti-angiogenesis effect of a corresponding anti-cancer treatment in an *in vivo* tumor model.

Conclusions

The tumor uptake of **6** was clearly visible; it was significantly higher than that in the contralateral background at all time points, and it demonstrated integrin-targeting specificity and high metabolic stability. In addition, **7** showed significantly

high tumor accumulation and desirable tumor to liver ratios for a radiotherapeutic purpose. Optimization of integrin $\alpha_v\beta_3$ expression therapy for human tumors will ultimately require further xenografts; however, the pharmacokinetic behavior of **7** described here holds considerable promise. The results of our *ex vivo* biodistribution and *in vivo* SPECT imaging studies, including a sensitive visibility in tumor xenograft presented here, suggest that the two agents that we have developed, ^{99m}Tc - and ^{188}Re -IDA-D-[c(RGDfK)]₂, hold promise as radiotheranostics in the field of tumor-induced angiogenesis.

Experimental

General

All commercial reagents and solvents were used without further purification unless otherwise specified. Reagents and solvents were commercially purchased from Sigma-Aldrich (Seoul, Korea). Flash column chromatography was performed with silica gel (230–400 mesh, ASTM; Merck). All reactions were monitored on pre-coated plates (silica gel 60F₂₅₄; Merck). NMR spectra were recorded on a Varian 400-MR (Palo Alto, CA, USA) spectrometer at ambient temperature. Chemical shifts were reported in parts per million (ppm, δ units). Electrospray ionization (ESI) was obtained on a Varian 500-MS ion trap mass spectrometer (Varian, Palo Alto, CA, USA) and MALDI-TOF mass spectra were performed on a Voyager-DE STR MALDI-TOF mass spectrometer (San Francisco, CA, USA). HPLC was carried out on a Thermo Separation Products System (Fremont, CA, USA) equipped with a semi-preparative column (Eclipse XDB-C18 column 5 μm , 9.4 \times 250 mm; Agilent Co., Palo Alto, CA, USA). Chromatography systems were fitted with a UV detector (SectraSystem UV3000 set at 214 nm; Thermo, Fremont, USA) and a gamma-ray detector (Flow-Count fitted with a NaI(Tl) detector; Bioscan, Washington DC, USA). Thin Layer Chromatography (TLC) of radiosynthesis was performed using Merck F₂₅₄ silica plates and analyzed on a Bioscan radio-TLC scanner (Washington DC, USA). All radio-activities were measured using a VDC-505 activity calibrator from Veenstra Instruments (Joure, The Netherlands). The cyclic pentapeptides, *i.e.*, cyclic-Arg(Pbf)-Gly-Asp(OtBu)-D-Phe-Lys-NH₂, cyclic-Arg(Pbf)-Ala-Asp(OtBu)-D-Phe-Lys-NH₂ (for ^{99m}Tc -IDA-D-[c(RADfK)]₂, details of observation and analysis appear in the online Supplementary Information†), and cyclic-Arg-Gly-Asp-D-Tyr-Val (for RGD[¹²⁵I]yV) were prepared using a solid support coupling protocol according to previously described methods.^{21,27} We purchased $^{99}\text{Mo}/^{99m}\text{Tc}$ - and $^{188}\text{W}/^{188}\text{Re}$ -generator from Samyoung Unitech (Seoul, Korea) and Enviro Korea (Daejeon, Korea), respectively.

Benzyl 1-amino-3,6,9,12-tetraoxapentadecan-15-oate (**8**)

A stirred solution of 1-[*N*-(*tert*-butyloxycarbonyl)-amino]-3,6,9,12-tetraoxapentadecanoic acid (224 mg, 0.61 mmol) and cesium carbonate (596 mg, 1.83 mmol) in acetonitrile (CH₃CN, 1 mL) at room temperature was treated with benzyl chloride (0.21 mL, 1.83 mmol) under argon atmosphere. The reaction mixture was warmed to 80 °C for 30 min. After cooling to room temperature, the reaction solvent was evaporated and the

crude mixture was purified by silica gel flash column chromatography using 5% MeOH-CH₂Cl₂ as the eluant, and combined benzylate in dichloromethane (CH₂Cl₂, 10 mL) was added in trifluoroacetic acid (1 mL) at 0 °C. The reaction mixture was stirred for 1 h at room temperature and basified by saturated sodium bicarbonate (25 mL). After extraction with CH₂Cl₂ (100 mL × 3), the combined organic layers were concentrated, and purified by silica gel flash column chromatography using MeOH-CH₂Cl₂-triethylamine (5 : 93 : 2) as the eluant, affording 194 mg (81%) of the title compound **8** as a pale yellow oil: ¹H NMR (400 MHz, CDCl₃) δ 7.38–7.33 (m, 5H), 5.14 (s, 2H), 3.78 (t, *J* = 6.2 Hz, 2H), 3.65–3.62 (m, 12H), 3.58 (t, *J* = 4.8 Hz, 2H), 2.93 (brs, 2H), 2.66 (t, *J* = 6.2 Hz, 2H), 2.51 (brs, 2H); ¹³C NMR (100 MHz, CDCl₃) δ 172.2, 135.6, 128.6, 128.4, 128.2, 70.3, 70.0 (× 3), 69.85, 69.79, 66.9, 66.7, 66.5, 39.8, 34.7; MS (ESI) *m/z* 356 (M + H)⁺; HRMS calcd for C₁₈H₃₀NO₆ 356.2068, found 356.2052.

2-[Bis(2-*tert*-butoxy-2-oxoethyl)amino]acetic acid (**10**)

A stirred solution of glycine methyl ester hydrochloride (**9**, 500 mg, 3.98 mmol) and *N,N'*-diisopropylethylamine (DIEA, 2.10 mL, 11.9 mmol) in CH₃CN (5 mL) at room temperature was treated with *tert*-butyl bromoacetate (1.76 mL, 11.9 mmol). After the mixture was stirred at 60 °C for 12 h, the cooled solution was concentrated *in vacuo* and extracted with ethyl acetate (EtOAc, 100 mL × 3). After the combined organic layers were dried and concentrated, a solution of the crude product in methanol (MeOH, 10 mL) was treated with a 1 M LiOH solution (2.0 equiv.) and stirred at 50 °C for 1 h. After the cooled solution was concentrated *in vacuo*, the residue was dissolved in water and acidified to pH 5 with 1 M HCl and extracted with EtOAc (100 mL × 3). The combined organic layers were concentrated, and purified by silica gel flash column chromatography using 5% MeOH-CH₂Cl₂ as the eluant, affording 603 mg (50%) of the title compound **10** as a white solid: mp 117–124 °C; ¹H NMR (400 MHz, CDCl₃) δ 3.49 (s, 2H), 3.47 (s, 4H), 1.48 (s, 18H); ¹³C NMR (100 MHz, DMSO-*d*₆) δ 172.3, 169.9, 80.3, 55.2, 54.5, 27.8; MS (ESI) *m/z* 304 (M + H)⁺; HRMS calcd for C₁₄H₂₆NO₆ 304.1755, found 304.1750.

6-(2-*tert*-Butoxy-2-oxoethyl)-2,2-dimethyl-4,8-dioxo-3,12,15,18,21-pentaoxa-9-azatetracosan-24-oic acid (**11**)

A stirred solution of compound **10** (60 mg, 0.19 mmol), 1-hydroxybenzotriazole (HOBT, 51 mg, 0.38 mmol) and *O*-benzotriazole-*N,N,N',N'*-tetramethyl-uronium-hexafluorophosphate (HBTU, 144 mg, 0.38 mmol) in *N,N'*-dimethylformamide (DMF, 5 mL) at room temperature was treated with the mixture of compound **8** (47 mg, 0.13 mmol) and DIEA (133 μL, 0.76 mmol) *via* dropwise addition. The resulting solution was stirred for 16 h at room temperature, and then the solvent was removed *in vacuo*. The crude reaction mixture was purified by silica gel flash column chromatography using 5% MeOH-CH₂Cl₂ as the eluant. A solution of the crude product in methanol (5 mL) was treated with 10% palladium on charcoal (2.0 equiv.) under nitrogen atmosphere. After gas atmosphere was exchanged from N₂ to H₂ gas, the reaction mixture was stirred for 16 h at room temperature. The reaction mixture was filtered through a Celite layer and then the solvent was removed *in vacuo*. The

desired compound **11** (120 mg, 76%) was obtained as a colorless oil: ¹H NMR (400 MHz, CDCl₃) δ 9.02 (brs), 8.20 (brs), 3.75–3.70 (m, 2H), 3.63–3.56 (m, 14H), 3.52–3.47 (m, 2H), 3.38–3.36 (m, 6H), 2.57 (t, *J* = 6.0 Hz, 2H), 1.44 (s, 18H); ¹³C NMR (100 MHz, CDCl₃) δ 175.0, 171.8, 170.5, 81.7, 70.34, 70.32, 70.29, 70.2, 70.10, 70.06, 69.8, 67.0, 58.8, 56.6, 38.8, 35.5, 28.1; MS (ESI) *m/z* 551 (M + H)⁺; HRMS calcd for C₂₅H₄₇N₂O₁₁ 551.3174, found 551.3158.

N-α-Bis(*tert*-butoxycarbonylmethyl)-aspartic acid dibenzyl ester (**13**)

To a solution of L-aspartic acid dibenzyl ester (**12**, 1 g, 2.85 mmol) and DIEA (1.5 mL 8.57 mmol) in CH₃CN (15 mL), *tert*-butylbromoacetate (1.27 mL, 8.57 mmol) was added at 90 °C under nitrogen gas. After the reaction mixture was refluxed for 12 h, the solvent was removed *in vacuo*, and the residue was dissolved in EtOAc (100 mL), the organic solution was washed with saturated sodium chloride (30 mL), followed by water (30 mL) and dried over anhydrous sodium sulfate. The organic solution was concentrated, and purified by silica gel flash column chromatography using 20% EtOAc-hexane as the eluant, affording 770 mg (50%) of the title compound **13** as a colorless oil: ¹H NMR (400 MHz, CDCl₃) δ 7.36–7.26 (m, 10H), 5.14–5.06 (m, 4H), 3.99 (dd, *J* = 9.2, 5.2 Hz, 1H), 3.61–3.50 (m, 4H), 2.94 (dd, *J* = 16.8, 9.6 Hz, 1H), 2.82 (dd, *J* = 16.4, 5.6 Hz, 1H), 1.42 (s, 18H); ¹³C NMR (100 MHz, CDCl₃) δ 171.2, 170.6, 170.5, 135.74, 135.66, 128.48, 128.46, 128.24, 128.22, 128.18, 128.13, 81.0, 66.7, 66.5, 61.0, 53.5, 35.9, 28.1; MS (FAB) *m/z* 542 (M+H)⁺; HRMS calcd for C₃₀H₄₀NO₈ 542.2754, found 542.2751.

N-α-Bis(*tert*-butoxycarbonylmethyl)-aspartic acid (**14**)

A solution of compound **13** (460 mg, 0.85 mmol) in methanol (10 mL) was treated with 10% palladium on charcoal (2.0 equiv.) under nitrogen atmosphere. After gas atmosphere was exchanged from N₂ to H₂ gas, the reaction mixture was stirred for 12 h at room temperature. The reaction mixture was filtered through a Celite layer and then the solvent was removed *in vacuo*. The desired compound **14** (278 mg, 91%) was obtained as a colorless oil: ¹H NMR (400 MHz, CDCl₃) δ 9.60 (brs, 2H), 3.90 (t, *J* = 6.6 Hz, 1H), 3.55–3.40 (m, 4H), 2.98 (dd, *J* = 16.4, 5.2 Hz, 1H), 2.66 (dd, *J* = 16.8, 7.6 Hz, 1H), 1.46 (s, 18H); ¹³C NMR (100 MHz, CDCl₃) δ 175.3, 174.6, 172.3, 82.7, 62.7, 54.2, 34.4, 28.0; MS (EI) *m/z* 361 (M+H)⁺; HRMS calcd for C₁₆H₂₇NO₈ 361.1736, found 361.1738.

N-α-Bis(hydroxycarbonylmethyl)-cyclic(Arg-Gly-Asp-D-Phe-Lys), IDA-c(RGDFK) (**16**)

A stirred solution of cyclic[Arg(Pbf)-Gly-Asp(OtBu)-D-Phy-Lys-NH₂] (**15**, 240 mg, 0.26 mmol) and DIEA (130 μL, 0.77 mmol) in CH₃CN (5 mL) was treated with *tert*-butyl bromoacetate (115 μL, 0.77 mL) in CH₃CN (1 mL). The resulting solution was stirred at 50 °C for 12 h and then the cooled solution was evaporated under reduced pressure. The crude reaction mixture was purified by silica gel flash column chromatography using 10% MeOH-CH₂Cl₂ as the eluant, affording the protected peptide, *N*-α-bis(*tert*-butyloxycarbonylmethyl)-cyclic[Arg(Pbf)-Gly-Asp(OtBu)-D-Phy-Lys], as a colorless oil; MS (MALDI) *m/z* 1163 (M + Na)⁺. Subsequently, the obtained peptide was treated with a solution of trifluoroacetic acid-

HSCH₂CH₂SH–water (5 mL, 95 : 2.5 : 2.5). The reaction mixture was stirred for 24 h at room temperature and then the solution was evaporated *in vacuo*. To get the solid, excess diethyl ether was added to the residue mixture. The resulting solid was filtered and washed with diethyl ether. After the solid dried under reduced pressure, it gave compound **16** (134 mg, 74%) as a white solid: MS (MALDI) *m/z* 720.8 (M + Na)⁺.

***N*-α-Bis(hydroxycarbonylmethyl)-PEG-cyclic(Arg-Gly-Asp-D-Phe-Lys), IDA-PEG-c(RGDfK) (17)**

To a solution of compound **11** (50 mg, 0.089 mmol), HOBT (36 mg, 0.27 mmol), and HBTU (100 mg, 0.27 mmol) in DMF (7 mL) was added a mixture of compound **15** (51 mg, 0.089 mmol) and DIEA (93 μL, 0.534 mmol) in DMF (3 mL) at room temperature under nitrogen gas. After the reaction mixture was stirred for 12 h, the solvent was removed under reduced pressure. The crude reaction mixture was purified by silica gel flash column chromatography using 10% MeOH/CH₂Cl₂ as eluant, affording the protected peptide, *N*-α-bis(*tert*-butyloxycarbonylmethyl)-PEG-cyclic[Arg(Pbf)-Gly-Asp(OtBu)-D-Phy-Lys], as a white solid; MS (ESI) *m/z* 1444.7 (M + H)⁺. Subsequently, deprotection and purification of the protected peptide were followed using the same conditions as described above in the method for compound **16**. After the solid dried under reduced pressure, it gave compound **17** (62 mg, 69%) as a white solid: MS (ESI) *m/z* 1024.5 (M + H)⁺.

***N*-α-Bis(hydroxycarbonylmethyl)-D-[cyclic(Arg-Gly-Asp-D-Phe-Lys)]₂, IDA-D-[c(RGDfK)]₂ (18)**

To a solution of compound **14** (39.5 mg, 0.11 mmol), HOBT (59.4 mg, 0.44 mmol), and HBTU (167 mg, 0.44 mmol) in DMF (7 mL) was added a mixture of compound **15** (350 mg, 0.38 mmol) and DIEA (153 μL, 0.88 mmol) in DMF (3 mL) at room temperature under nitrogen gas. After the reaction mixture was stirred for 12 h, the solvent was removed under reduced pressure. The crude reaction mixture was purified by silica gel flash column chromatography using 10% MeOH–CH₂Cl₂ as the eluant, affording the protected peptide, *N*-α-bis(*tert*-butyloxycarbonylmethyl)-D-[cyclic[Arg(Pbf)-Gly-Asp(OtBu)-D-Phy-Lys]]₂, as a white solid; MS (MALDI) *m/z* 2171.06 (M + Na)⁺. Subsequently, deprotection and purification of the protected peptide were followed using the same conditions as described above in the method for compound **16**. After the solid dried under reduced pressure, it gave compound **18** (97 mg, 62%) as a white solid: MS (ESI) *m/z* 1420.5 (M + H)⁺.

^{185/187}Re-IDA-RGD analogs (1–3)

To a solution of compounds **16**, **17** or **18** (10 μmol) in a solution of water (0.5 mL) and MeOH (0.5 mL) was added (NEt₄)₂[^{185/187}ReCl₃(CO)₃] (9.1 mg, 15 μmol). The reaction mixture was stirred at 60 °C for 3 h. The solution was removed under reduced pressure and then the product was purified by semi-preparative HPLC (Agilent Co. Eclipse XDB-C18 column; 5 μm, 9.4 × 250 mm). The column was eluted with a solvent mixture of CH₃CN–water–0.1% trifluoroacetic acid using a gradient condition. The HPLC eluent started with 20% CH₃CN–water (0.1% trifluoroacetic acid) from 0 to 5 min and the ratio was increased with a solvent mixture of 60% CH₃CN–water (0.1% trifluoroacetic acid) over 40 min. The effluent

from the column was monitored with a 214 nm UV detector. The chemically pure ^{185/187}Re-IDA-RGD analogs eluted with a retention time of 21.8 min for **1**, 22.1 min for **2** and 19.2 min for **3**. The product isolated from semi-preparative HPLC was diluted with excess water, passed through a tC₁₈ Sep-Pak cartridge, washed with water (5 mL) and eluted with methanol (2 mL). After methanol was removed under reduced pressure, it gave ^{185/187}Re-IDA-RGD analogs (**1**, **2**, and **3**, 60–78%) as a white solid: MS (ESI) *m/z* 990.85 (M + H)⁺ for **1**, MS (MALDI) *m/z* 1293.4 (M + H)⁺ for **2** and MS (ESI) *m/z* 1688.5 (M + H)⁺ for **3**.

General method for ^{99m}Tc-IDA-RGD analogs (4–6)

The *fac*-[^{99m}Tc(H₂O)₃(CO)₃]⁺ synthon was prepared according to Alberto *et al.*^{11,12} A solution of [^{99m}Tc(H₂O)₃(CO)₃]⁺ (370–740 MBq) in saline (200 μL) was added to the precursor (**16**, **17** or **18**, 0.3 mg) in water (300 μL). The reaction mixture was stirred at 75 °C for 30 min and then cooled in an ice bath. The radiotracer was purified by semi-preparative HPLC (Agilent Co. Eclipse XDB-C18 column; 5 μm, 9.4 × 250 mm) and used the same gradient condition as described in the general method for ^{185/187}Re-IDA-RGD analogs. The effluent from the column was monitored with a 214 nm UV detector followed by a gamma radioactive detector. The radiochemically pure **1**, **2**, or **3** eluted off with a retention time of 20.6 min for **1**, 21.4 min for **2** and 18.4 min for **3**, and the radiochemical yield ranged between 72–79%. The product isolated from semi-preparative HPLC was diluted with excess water, passed through a tC₁₈ Sep-Pak cartridge and washed with water (5 mL). The desired product was eluted by 80% ethanol–saline (1.5 mL) and evaporated under a stream of nitrogen gas. The product was made with saline and sterilized by passing through a sterile filter (0.22 μm).

General method for ¹⁸⁸Re-IDA-D-[c(RGDfK)]₂ (7)

The *fac*-[¹⁸⁸Re(H₂O)₃(CO)₃]⁺ was prepared according to the literature.¹³ To a solution of [¹⁸⁸Re(H₂O)₃(CO)₃]⁺ (50–100 mCi) in saline (200 μL) was added the precursor **18** (0.5 mg, 0.35 μmol) in water (300 μL). The reaction mixture was stirred at 75 °C for 60 min and then cooled in an ice bath. The radiotracer was purified by semi-preparative HPLC (Agilent Co. Eclipse XDB-C18 column; 5 μm, 9.4 × 250 mm) with the same gradient condition as described above. The effluent from the column was monitored with a 214 nm UV detector followed by a gamma radioactive detector. The radiochemically pure ¹⁸⁸Re-IDA-D-[c(RGDfK)]₂ eluted with a retention time of 19.2 min and the radiochemical yield ranged 50–55%. The product isolated from semi-preparative HPLC was diluted with excess water, passed through a tC₁₈ Sep-Pak cartridge and washed with water (5 mL). The desired product was eluted by 80% ethanol–saline (1.5 mL) and evaporated under a stream of nitrogen gas. The product was made isotonic with sodium chloride and sterilized by passing through a sterile filter (0.22 μm). Specific radioactivity of ¹⁸⁸Re-IDA-D-[c(RGDfK)]₂; 3.3 Ci/μmol was obtained after purification in an HPLC column.

Cell lines and animal model

For the *in vitro* competitive binding assay, U87-MG cells (ATCC) were cultured in Dulbecco's modified Eagle's medium supplemented with 4 mM L-glutamine, 4500 mg L⁻¹ glucose, 1

mM sodium pyruvate, 1.5 g mL⁻¹ sodium bicarbonate, 10% FBS and antibiotic-antimycotic (Gibco, Grand Island, NY, USA) at 37 °C in a humidified atmosphere of 5% CO₂. Human glioblastoma U87-MG cells were cultured for 2–3 days, without changing the media, and harvested with trypsin-EDTA in PBS. We resuspended the U87-MG cells (5 × 10⁶) in 100 μL with 100 mM PBS (pH 7.4) and injected them subcutaneously into the right shoulder of 6–7 week-old male Balb/c nu/nu mice (Orient Bio Inc., Seongnam, Korea). Animal protocols were approved by the Seoul National University Bundang Hospital Animal Care and Use Committee. We also performed caliper measurements of the longest perpendicular tumor diameters.

In vitro integrin receptor-binding assay

The receptor binding affinity studies of ^{185/187}Re-IDA-RGD analogs (**1**, **2**, and **3**) were performed using ¹²⁵I-c(RGDyV) as the integrin-specific radio-ligand in integrin α_vβ₃-positive human glioblastoma U87-MG cells. One hundred microliters of a cell suspension (10⁵ glioma cells) in Eppendorf tubes were incubated with ¹²⁵I-c(RGDyV) (0.037 MBq/tube) in the presence of increasing concentrations of cold (^{185/187}Re) RGD analogs. Tubes were centrifuged for 5 min at 2000 rpm at 4 °C. After removing the unbound ¹²⁵I-c(RGDyV), centrifuged cell pellets were washed three times with cold PBS (1 mL). The radioactivity was determined using a gamma counter (Perkin Elmer, wizard 1480, Turku, Finland). The IC₅₀ values were calculated by fitting the data by nonlinear regression using GraphPad Prism™ (GradPad Software, Inc., San Diego, CA). Experiments were carried out three times with triplicate samples. IC₅₀ values are reported as an average plus/minus the standard deviation in Chart 1.

Ex vivo distribution

Tissue biodistribution studies were performed in 6 week-old male nude mice, who were injected subcutaneously with 5 × 10⁶ U87-MG cells into the right shoulder. After tumor volume reached 62.8 ± 16.8 mm³ at 2 weeks post cell inoculation, mice were injected with ^{99m}Tc or ¹⁸⁸Re-IDA-RGD analogs (0.74 MBq, 200 μL in saline) into the tail vein, sacrificed at the indicated time points (*n* = 4, 10, 30, 60, 120, and 240 min post-injection for **4–6**; 10, 30, 60, 120, and 480 min post-injection for **7**). Blood, tumor, normal organs (liver, lung, spleen, kidneys, small intestine, large intestine, thyroid, brain), and muscle were promptly extracted and measured for radioactivity using a gamma counter (PerkinElmer, Wellesley, MA, USA). Radioactivity in the organs was presented as the percentage of the injected dose per gram of tissue in comparison with samples of a standard dilution of the initial dose (% ID/g).

Metabolic stability studies

The metabolic stability of ^{99m}Tc-IDA-D-[c(RGDfK)]₂ (**6**) was evaluated in the tumor-bearing mice. U87-MG-bearing mice injected *via* the tail vein with ^{99m}Tc-IDA-D-[c(RGDfK)]₂ (37 MBq) were subsequently sacrificed and dissected at 0.5 and 2 h post-injection. Blood was immediately centrifuged for 5 min at 3500 rpm at 4 °C and the serum supernatant was collected. The liver, kidneys, and tumors were each homogenized with cold PBS (2 mL) in an ice chamber and centrifuged for 5 min at

3500 rpm at 4 °C. After removal of the supernatant, the pellets were washed twice with cold PBS (2 mL). For each sample, the supernatants of both centrifugation steps for the blood, liver, kidneys, and tumor were combined and passed through tC-18 Sep-Pak cartridges. The urine samples were diluted with 2 mL of cold PBS and passed through a tC-18 Sep-Pak cartridge, and the cartridge was washed with 2 mL of water and eluted with CH₃CN (3 mL). Then, organic fractions (400 μL) were diluted with water (1.6 mL), and the aliquots were analyzed by HPLC. The identification of the percentage of the intact tracer was performed using RP-HPLC (YMC C18, 5 μm, 7.9 × 250 mm) with a 25% CH₃CN–water–0.1% trifluoroacetic acid gradient (2 mL min⁻¹, *t_R* = 19.5 min).

CT procedure

An animal CT scanner system (NanoSPECT/CT, Bioscan Inc., Washington DC) consisting of a low-energy X-ray tube (X-ray energy, 45 kVp, 177 μA; 180 projections) and a precision-motion translation stage was used. The detector and X-ray source rotate about a fixed bed, allowing the mouse to be kept in the same horizontal position in the CT scanner as in the SPECT scanner. The images were acquired with the X-ray source set at 45 kVp and 177 μA. Two-dimensional slices of the bed position were reconstructed using an Exact Cone Beam Filter Back Projection (FBP) algorithm with a Shepp-Logan filter. The CT images were reconstructed on a voxel–pixel size of 0.20 : 0.192 mm, providing image sizes (*x, y, z*) of 176 × 176 × 136 with an image resolution of 48 μm. For reconstruction in Hounsfield units, the system was calibrated using a 50 mL polypropylene tube filled with water.

SPECT/CT imaging

We performed SPECT imaging studies when the tumor volume reached 81.8 ± 13.5 mm³. SPECT images and X-ray CT images were acquired using an animal SPECT/CT scanner system (NanoSPECT/CT, Bioscan Inc., USA). SPECT imaging was performed using a low-energy and high-resolution pyramid collimator. We obtained high-resolution scans (18 frames) of each mouse from 0 min to 180 min after the intravenous injection of radiotracers (**4–6** and ^{99m}Tc-IDA-[c(RADfK)]₂, 18.5 MBq, *n* = 3). Mice were placed in a prone position on the bed under anesthesia with 2% isoflurane. On the anesthetized mouse, whole body images were obtained in 24 projections over a 10 min period using a 4-head scanner with 4 × 9 (1.4 mm) pinhole collimators in helical scanning mode. The X-ray source and detectors are mounted on a circular gantry allowing it to rotate 360° around the mouse positioned on a stationary bed. The energy window was set at 140 KeV ± 15%. SPECT imaging was followed by CT image acquisition with the animal in exactly the same position. The software programs HisSPECT version 1.0 (Bioscan Inc.) and InVivoScope version 1.43 (Bioscan Inc.) were used for image reconstruction and quantification, respectively. The SPECT images were reconstructed to produce an image size (*x, y, z*) of 176 × 176 × 136 with a voxel size (*x, y, z*) of 0.2 × 0.2 × 0.2 mm. Images of ^{99m}Tc-labeled compounds in Fig. 1 and 2 were obtained at a mid-scan time of 25 min, for a scan duration of 10 min in tumor-bearing nude mice.

In the SPECT/CT image of 7 (37 MBq), a whole body image was obtained according to the similar acquisition protocol of 4–6 except for 12 projections over a 30 min period with 155 KeV \pm 15% of the energy window. The image of 7 in Fig. 1 was obtained at a mid-scan time of 45 min, for a scan duration of 30 min in tumor-bearing nude mice. The accumulated radioactivity of $^{99m}\text{Tc}/^{188}\text{Re}$ -IDA-RGD analogs in the tumor at the specified time-points was extracted from the images by drawing regions of interest (ROI) using the 37–55.5 MBq radioactivity of ^{99m}Tc and ^{188}Re as a reference source. The percentage of the injected dose per gram of weight (% ID/g) was determined from the radioactivity in the ROI on the tumor after intravenous injection of $^{99m}\text{Tc}/^{188}\text{Re}$ -compounds, with the location of the edge of the ROI being the contour for 70% of the maximum intensity.

Acknowledgements

This work was supported by the National Research Foundation of Korea (NRF) grant funded by the Korea government (MEST) (20110018410, 20110030953, 20110006321) and the grant of the Korea Healthcare Technology R&D Project, Ministry of Health and Welfare, Republic of Korea (A102158).

References

- M. H. Michalski and X. Chen, *Eur. J. Nucl. Med. Mol. Imaging*, 2011, **38**, 385.
- L. Fass, *Mol. Oncol.*, 2008, **2**, 115.
- P. C. Brooks, A. M. Montgomery, M. Rosenfeld, R. A. Reisfeld, T. Hu, G. Klier and D. A. Cheresch, *Cell*, 1994, **79**, 1157.
- M. Gurrath, G. Muller, H. Kessler, M. Aumailley and R. Timpl, *Eur. J. Biochem.*, 1992, **210**, 911.
- E. Ruoslahti and M. D. Pierschbacher, *Cell*, 1986, **44**, 517.
- R. Haubner, H. J. Wester, W. Weber, C. Mang, S. L. Ziegler and S. L. Goodman, *Cancer Res.*, 2001, **61**, 1781.
- M. L. Janssen, W. I. Oyen, I. Dijkgraaf, L. F. Massuger, C. Frielink, S. Edwards, M. Rajopadhye, H. Boonstra, F. H. Corstens and O. C. Boerman, *Cancer Res.*, 2002, **62**, 6146.
- J. Shi, Y.-S. Kim, S. Chakraborty, B. Jia, F. Wang and S. Liu, *Bioconjugate Chem.*, 2009, **20**, 1559.
- C. Decristoforo, I. Santos, H. J. Pietzsch, J. U. Kuenstler, A. Duatti, C. J. Smith, A. Rey, R. Alberto, E. Von Guggenberg and R. Haubner, *Q. J. Nucl. Med. Mol. Imaging*, 2007, **51**, 33.
- J. Shi, Y.-S. Kim, S. Zhai, Z. Liu, X. Chen and S. Liu, *Bioconjugate Chem.*, 2009, **20**, 750.
- R. Alberto, R. Schibli, A. Egli, A. P. Schubiger, U. Abram and T. A. Kaden, *J. Am. Chem. Soc.*, 1998, **120**, 7987.
- R. Alberto, R. Schibli, R. Waibel, U. Abram and A. P. Schubiger, *Coord. Chem. Rev.*, **190–192**, 901.
- R. Schibli, R. Schwarzbach, R. Alberto, K. Ortner, H. Schmalle, C. Dumas, A. Egli and P. A. Schubiger, *Bioconjugate Chem.*, **13**, 750.
- R. Schibli, M. Netter, L. Scapozza, M. Birringer, P. Schelling, C. Dumas, J. Schoch and P. A. Schubiger, *J. Organomet. Chem.*, 2003, **668**, 67.
- B. C. Lee, D. H. Kim, J. H. Lee, H. J. Sung, Y. S. Choe, D. Y. Chi, K.-H. Lee, Y. Choi and B. T. Kim, *Bioconjugate Chem.*, 2007, **18**, 1332.
- S. Alves, J. D. G. Correia, L. Gano, T. L. Rold, A. Prasanphanich, R. Haubner, M. Rupprich, R. Alberto, C. Decristoforo, I. Santos and C. J. Smith, *Bioconjugate Chem.*, 2007, **18**, 530.
- B. L. Oliveira, P. D. Raposinho, F. Mendes, F. Figueira, I. Santos, A. Ferreira, C. Cordeiro, A. P. Freire and J. D. Correia, *Bioconjugate Chem.*, 2010, **21**, 2168.
- E.-M. Kim, M.-H. Joung, C.-M. Lee, H.-J. Jeong, S. T. Lim, M.-H. Sohn and D. W. Kim, *Bioorg. Med. Chem. Lett.*, 2010, **20**, 4240.
- L. Huang, H. Zhu, Y. Zhang, X. Xu, W. Cui, G. Yang and Y. M. Shen, *Steroids*, 2010, **75**, 905.
- K.-H. Jung, K.-H. Lee, J.-Y. Paik, B.-H. Ko, J.-S. Bae, B. C. Lee, H. J. Sung, D. H. Kim, Y. S. Chi and D. Y. Chi, *J. Nucl. Med.*, 2006, **47**, 2000.
- B. C. Lee, H. J. Sung, J. S. Kim, K.-H. Jung, Y. S. Choe, K.-H. Lee and D. Y. Chi, *Bioorg. Med. Chem.*, 2007, **15**, 7755.
- E. G. Garayoa, C. Schweinsberg, V. Maes, L. Brans, P. Bläuenstein, D. A. Tourwé, R. Schibli and P. A. Schubiger, *Bioconjugate Chem.*, 2008, **19**, 2409.
- Z. Liu, B. Jia, H. Zhao, X. Chen and F. Wang, *Mol. Imaging Biol.*, 2011, **13**, 112.
- H. Wang, K. Chen, W. Cai, Z. Li, L. He, A. Kashefi and X. Chen, *Mol. Cancer Ther.*, 2008, **7**, 1044.
- H. Akizawa, Y. Arano, M. Mifune, A. Iwado, Y. Saito, T. Mukai, T. Uehara, M. Ono, Y. Fujioka, K. Ogawa, Y. Kiso and H. Saji, *Nucl. Med. Biol.*, 2001, **28**, 761.
- L. Sancey, E. Garanger, S. Foillard, G. Schoehn, A. Hurbin, C. Albiges-Rizo, D. Boturnyn, C. Souchier, A. Grichine, P. Dumy and J. L. Coll, *Mol. Ther.*, 2009, **17**, 837.
- R. Haubner, H. J. Wester, U. Reuning, R. Senekowitsch-Schmidtke, B. Diefenbach, H. Kessler, G. Stöcklin and M. Schwaiger, *J. Nucl. Med.*, 1999, **40**, 1061.